Nozu *Earth, Planets and Space* (2023) 75:181
https://doi.org/10.1186/s40623-023-01936-y

Earth, Planets and Space

EXPRESS LETTER

Open Access

The region of large site amplification in Northern Hokkaido, Japan, extends to the eastern Soya Region

Atsushi Nozu[1*]

Abstract

In the document titled "predominant period of long-period ground motions and the natural period of deep subsoil" by the Central Disaster Management Council, the west part of Northern Hokkaido facing the Sea of Japan is categorized as a region, where long-period (> 6 s) ground motions are predominant. In contrast, the document categorizes the east part of Northern Hokkaido as a region where short-period (< 1 s) ground motions are predominant. The J-SHIS velocity structure model also implies that a deep sedimentary basin is located in the west part of Northern Hokkaido, but not in the east part. However, the result of a past generalized inversion analysis was inconsistent with these general understanding and suggested that the region of large site amplification in the low-frequency range in Northern Hokkaido extends to the eastern Soya Region. It was preferable to check this result with an independent dataset. Therefore, in this study, the records of the May 24, 2013, M_W8.3, Sea of Okhotsk earthquake were used to investigate the distributions of site amplification factors in Northern Hokkaido. Because this is a distant earthquake and the epicentral distance was greater than 1300 km even at the closest station in Hokkaido, it was assumed that the difference of ground motions at different stations represents the difference of the site effects. The Fourier spectra for the S wave part of this earthquake at K-NET and KiK-net stations clearly indicated that the region of large site amplification in the low-frequency range in Northern Hokkaido does extend to the eastern Soya Region. It is desirable in a future study to reveal the cause of the discrepancy between this amplification pattern and the existing velocity structure models.

Keywords Ground motion, Site effect, Northern Hokkaido, The 2013 Sea of Okhotsk earthquake, Sedimentary basin, Subsurface structure

*Correspondence:
Atsushi Nozu
nozu@p.mpat.go.jp
Full list of author information is available at the end of the article

Graphical Abstract

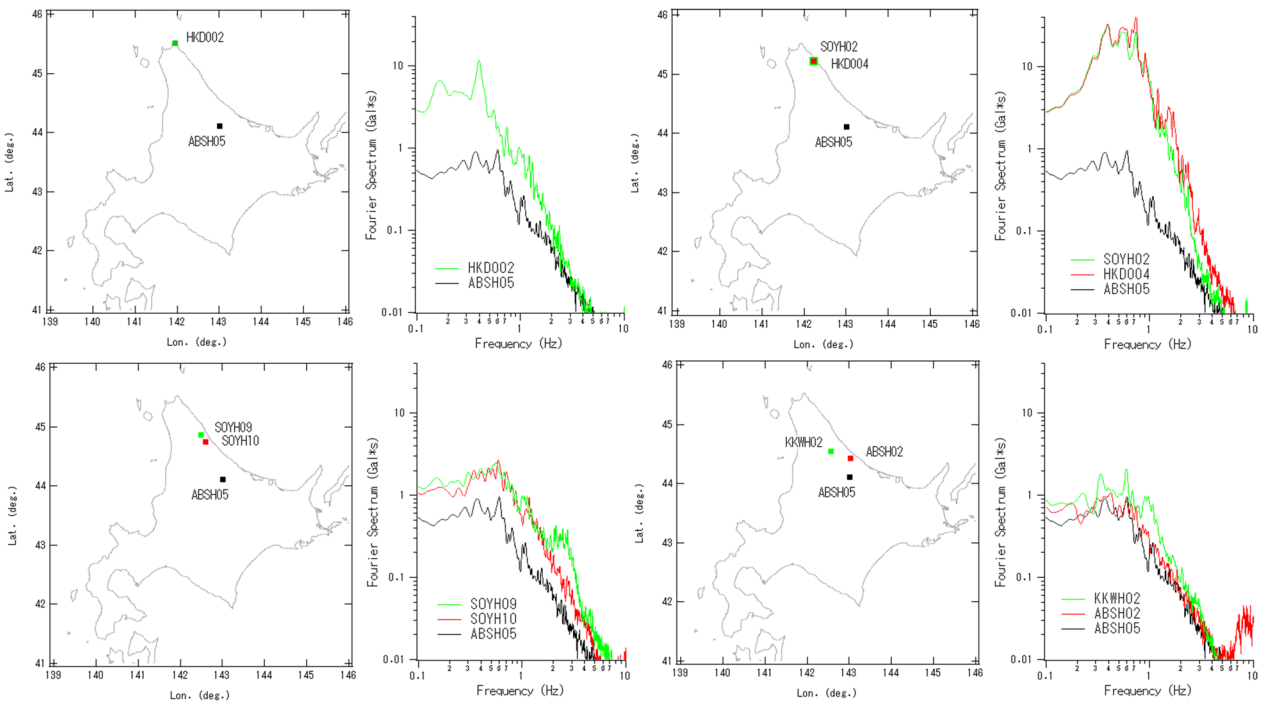

The Fourier spectra for the S wave part of the May 24, 2013, Mw8.3 Sea of Okhotsk earthquake at K-NET and KiK-net stations clearly indicated that the region of large site amplification in the low frequency range in Northern Hokkaido extends to the eastern Soya Region.

Introduction

It is of fundamental importance to consider the site-specific nature of earthquake ground motions in the design of infrastructures. There are approximately 1000 ports all over Japan and the author is interested in the site amplification factors at each of those ports. The ports in Hokkaido are also included in the author's scope.

It has been recognized that a deep sedimentary basin is located in the west part of Northern Hokkaido facing the Sea of Japan and the predominance of long-period ground motions is expected in that region just as it is expected in Yufutsu or Niigata Plains, Japan. In fact, according to the document titled "the predominant period of long-period ground motions and the natural period of deep subsoil" prepared by the Japanese government (Central Disaster Management Council 2008), the west part of Northern Hokkaido is allocated to red or pink regions in their Fig. 4.20, indicating that long-period (> 6 s) ground motions are predominant in that region. However, in their document, the east part of Northern Hokkaido facing the Sea of Okhotsk is allocated to a dark-blue region, indicating that short-period (< 1 s) ground motions are predominant. This map will be hereinafter referred to as the CDMC map.

Fujiwara et al. (2009) developed a velocity structure model for Japan for use in developing national seismic hazard maps and published through a website called the "Japan Seismic Hazard Information Station (J-SHIS)". This velocity structure model will be referred to as the J-SHIS model in this article. The J-SHIS model also implied that a deep sedimentary basin is located in the west part of Northern Hokkaido, but not in the east part.

On the other hand, Nozu and Sugano (2010) applied a spectral inversion analysis (Iwata and Irikura 1986), hereinafter referred to as the "GIT analysis", to strong motion records of K-NET and KiK-net (Aoi et al 2020) in Northern Hokkaido to evaluate site amplification factors. Their analysis resulted in large site amplification factors in the low-frequency range of 0.2–1 Hz in the west part of Northern Hokkaido, which was consistent with the CDMC map and the J-SHIS model. However, their analysis also indicated large site amplification factors in the low-frequency range of 0.2–1 Hz in the east part of Northern Hokkaido, facing the Sea of Okhotsk. This result was not consistent either with the CDMC map or with the J-SHIS model. The GIT analysis by Nozu and

Sugano (2010) was based on a limited number of events which were available when the study was conducted and, therefore, the results might have been influenced by, for example, the radiation pattern of individual events. Therefore, the author of this article was not confident with the large site amplification factors obtained in the east part of Northern Hokkaido.

On May 24, 2013, an M_W8.3 earthquake occurred in the Sea of Okhotsk at a depth of 598.1 km (USGS 2022). The earthquake was recorded at 471 K-NET and KiK-net stations extending from Hokkaido to Kyushu. Because this is a distant earthquake and the epicentral distance was greater than 1300 km even at the closest station in Hokkaido, it could be reasonable to assume the same source radiation pattern and the same attenuation along the propagation path among different strong motion stations in Hokkaido; it could be reasonable to assume that the difference of ground motions is due to the difference of the site effects. Therefore, in this study, the records of this earthquake were used for the purpose of validating the results obtained in Nozu and Sugano (2010) with special reference to the large site amplification in the low frequencies in the east part of Northern Hokkaido. Because of the large distance, the P and S waves are isolated from each other. Some stations recorded only P waves and other stations recorded only S waves. There were also stations that recorded both P and S waves. A special attention was paid to such difference. The result indicated that the region of large site amplification in the low-frequency range in Northern Hokkaido does extend to the eastern Soya Region.

Result of the previous GIT analysis

Before the analysis by Nozu and Sugano (2010), site amplification factors at 260 strong motion stations in Hokkaido were evaluated by Nozu and Nagao (2005). However, it was found afterwards that the site amplification factors at several sites in Northern Hokkaido were overestimated at around 0.2 Hz, because the records of one small event were contaminated by the later phases of a larger event that occurred 5 min before the small event. Therefore, Nozu and Sugano (2010) re-evaluated the site amplification factors for strong motion stations in Northern Hokkaido based on available records in the frequency range of 0.2–10.0 Hz. In the analysis, records from four earthquakes at 118 sites were used. To avoid the trade-off between the source spectra and the site amplification factors, the site amplification factors at three sites were constrained using the results of Nozu and Nagao (2005). The source spectra estimated in the analysis were in good agreement in the low-frequency range with the values of seismic moments in the F-net moment tensor solutions (NIED 2022), indicating the adequacy of the constraint used for the analysis.

As a result of the analysis, the site amplification factors at 115 sites were newly obtained. Figure 1a shows the comparison between the J-SHIS model and the site amplification factors at strong motion stations obtained in the GIT analysis. The color contour indicates the thickness of the layers with a shear wave velocity less than 2000 m/s in the J-SHIS model. Blue circles show stations with small site amplification factors less than 5 averaged over 0.2–0.3 Hz. Yellow circles show stations with large site amplification factors in the range of 5–20 averaged over 0.2–0.3 Hz. Red circles show stations with very large site amplification factors greater than 20 averaged over 0.2–0.3 Hz. The J-SHIS model indicates the existence of a deep sedimentary basin in the west part of Northern Hokkaido and the GIT analysis also resulted in large site amplification factors in the low-frequency range in that region. In that sense the results of the GIT analysis were consistent with the J-SHIS model and the CDMC map mentioned in the introduction. However, the GIT analysis indicated that the region of large site amplification in the low-frequency range in Northern Hokkaido extends to the eastern Soya Region. This result was not consistent either with the J-SHIS model or with the CDMC map.

The May 24, 2013 Sea of Okhotsk earthquake

On May 24, 2013, 14:44:48 JST (5:44:48 UTC), an M_W8.3 earthquake occurred in the Sea of Okhotsk, at 54.892°N and 153.221°E, at a depth of 598.1 km (Fig. 2). These parameters were determined by the USGS (2022). The earthquake was recorded at 471 K-NET and KiK-net

(See figure on next page.)

Fig. 1 Comparison between the J-SHIS velocity structure model (Version 1; Fujiwara et al. 2009) and the site amplification factors at strong motion stations; **a** the color contour indicates the thickness of the layers with a shear wave velocity less than 2,000 m/s in the J-SHIS model. The circles indicate the strong motion stations where the site amplification factors were evaluated by the GIT analysis (Nozu and Sugano 2010). Blue circles show stations with small site amplification factors less than 5 averaged over 0.2–0.3 Hz. Yellow circles show stations with large site amplification factors in the range of 5–20 averaged over 0.2–0.3 Hz. Red circles show stations with very large site amplification factors greater than 20 averaged over 0.2–0.3 Hz. **b** the same as (**a**) but the circles indicate the strong motion stations where the site amplification factors were evaluated in this study based on the records of the May 24, 2013, Mw8.3 earthquake. Blue circles show stations with small site amplification factors less than 5 averaged over 0.2–0.3 Hz. Yellow circles show stations with large site amplification factors in the range of 5–20 averaged over 0.2–0.3 Hz. Red circles show stations with very large site amplification factors greater than 20 averaged over 0.2–0.3 Hz

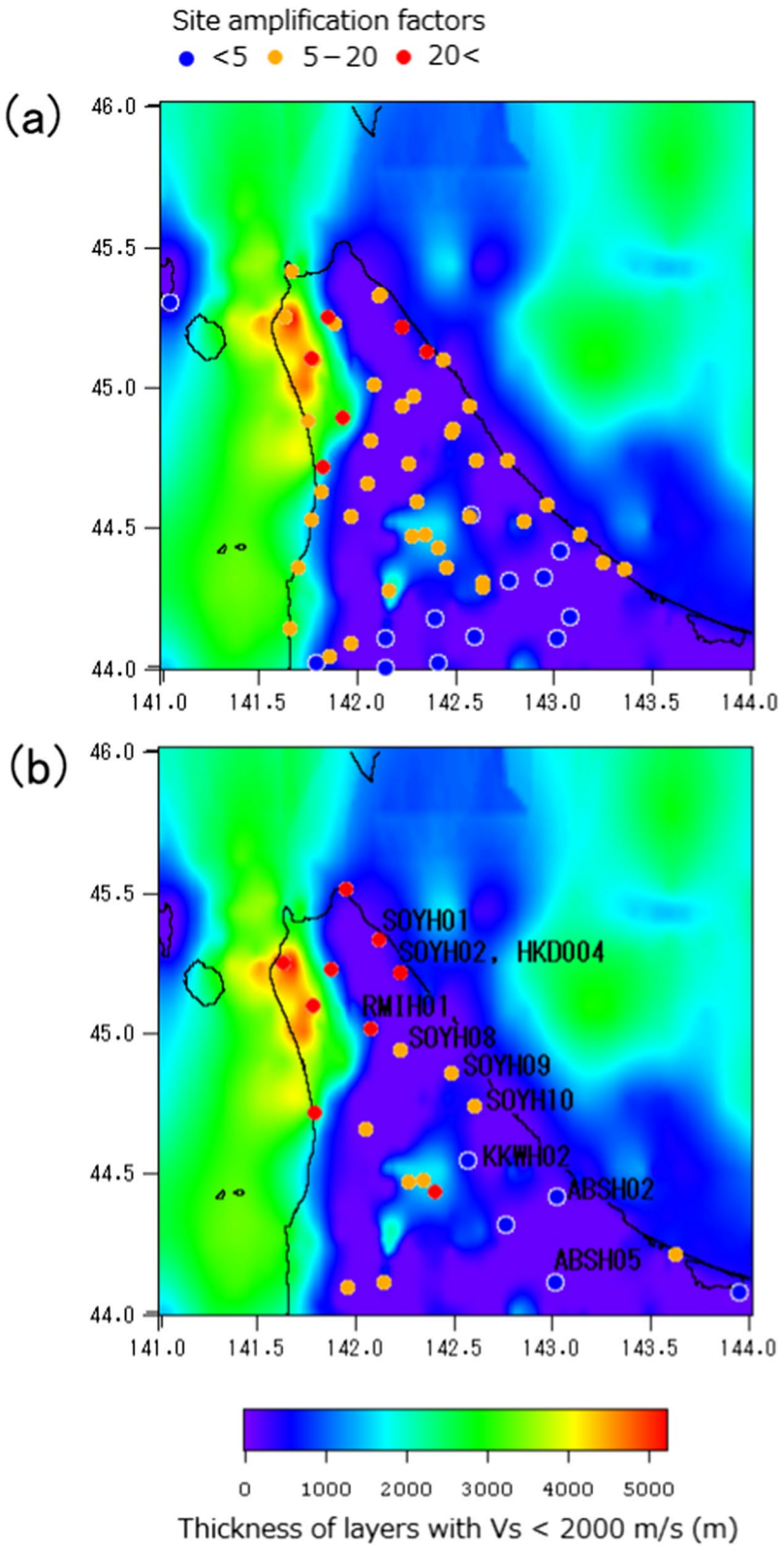

Fig. 1 (See legend on previous page.)

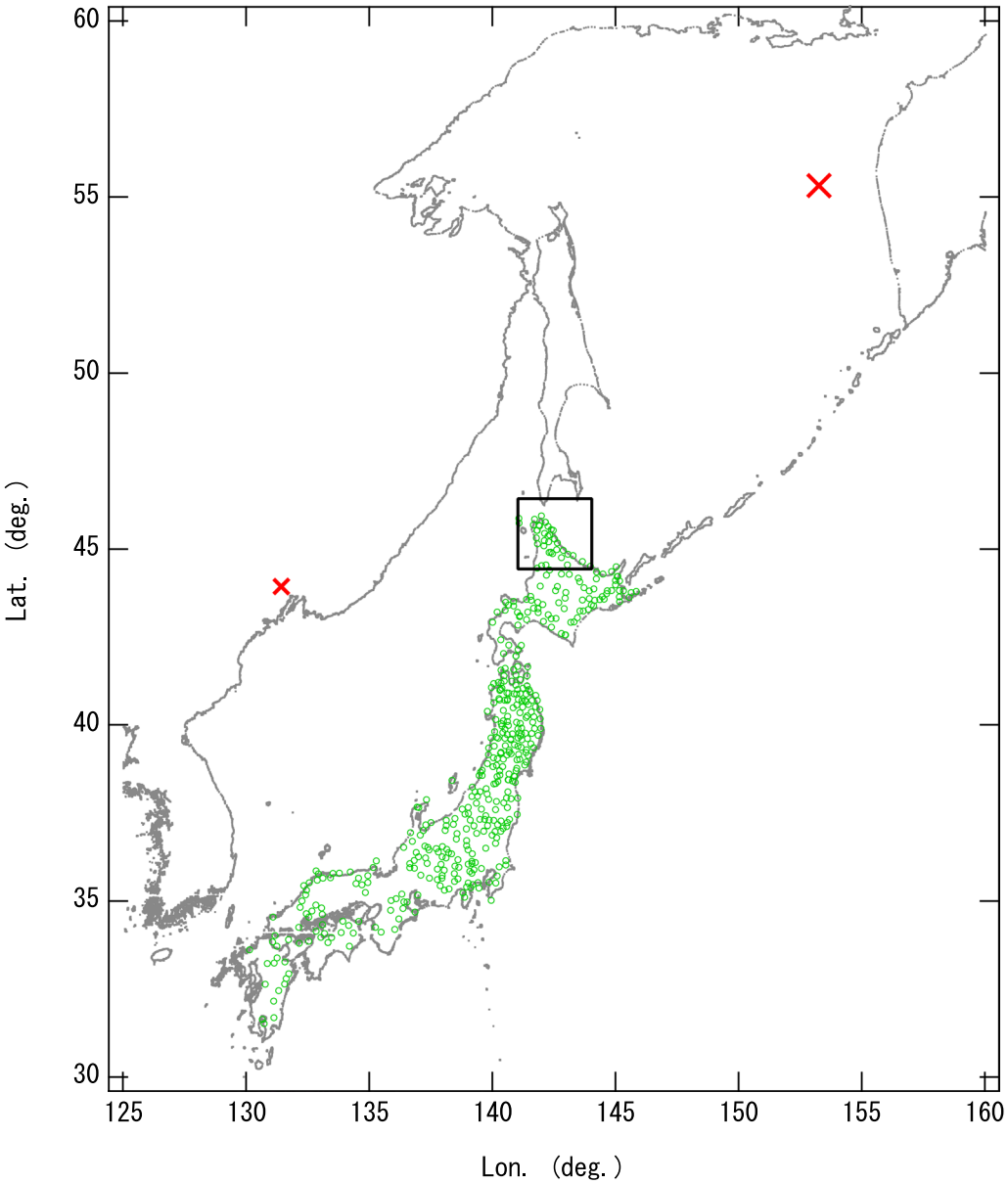

Fig. 2 The May 24, 2013 Sea of Okhotsk earthquake and the K-NET and Kik-net stations; The large cross shows the epicenter of the May 24, 2013 Sea of Okhotsk earthquake based on USGS (2022). The green circles show the K-NET and KiK-net stations that observed this earthquake. The black rectangle shows the region shown in Fig. 1. The small cross shows the epicenter of the June 29, 2002 Vladivostok earthquake based on the Japan Meteorological Agency

stations from Hokkaido to Kyushu as shown in Fig. 2. Because this is a distant earthquake and the epicentral distance was greater than 1300 km even at the closest station in Hokkaido, it could be reasonable to assume the same source radiation pattern and the same attenuation along the propagation path among different strong motion stations in Hokkaido; it could be reasonable to assume that the difference of ground motions is due to the difference of the site effects. Therefore, the records of this earthquake were used for the purpose of validating the results obtained in the GIT analysis.

Figure 3 shows the paste up of the acceleration waveforms for the May 24, 2013 Sea of Okhotsk earthquake. The KiK-net borehole accelerations are shown. Because of the large distance, the P and S waves are isolated from each other. Some stations recorded only P waves and other stations recorded only S waves. There were also stations that recorded both P and S waves. It can be also

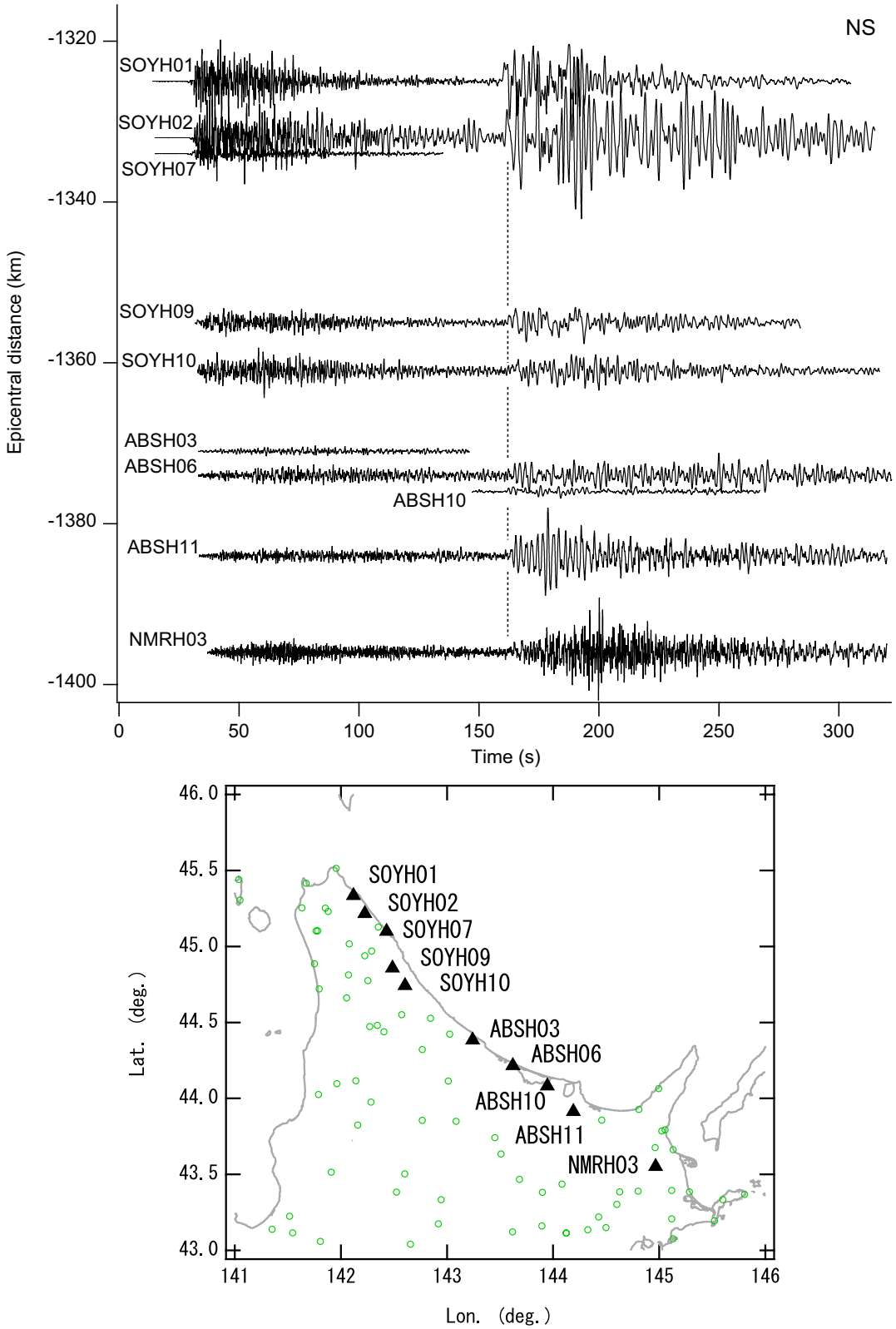

Fig. 3 Paste up of the acceleration waveforms for the May 24, 2013 Sea of Okhotsk earthquake; The top panel shows the paste up of the NS component acceleration waveforms observed at KiK-net stations along the Okhotsk Coast. The borehole accelerations are shown. The origin of the horizontal axis is 14:47:00 JST, which is 132 s after the origin time. The vertical axis shows the epicentral distance. The bottom panel shows the stations used for the paste up

observed that the initial S waves arrived at these stations almost simultaneously. It means that the wave front was almost parallel to the coast of Hokkaido facing the Sea of Okhotsk. If we consider the fact that these stations have slightly different epicentral distances, it could be reasonable to conclude that the seismic ray connecting the source and Hokkaido was not a simple straight line but was slightly rotated clockwise near Hokkaido. However, we can at least assume that much of the S wave energy was arriving from the source and not from, for example, the closest part of the Chishima Trench.

To understand the seismic wave contents arriving at the later portions of the paste up shown in Fig. 3, synthetic seismograms were calculated for the locations of SOYH01 and NMRH03 assuming a point source, using a layered subsurface structure model routinely used to obtain moment tensor solutions in Japan (Fukuyama et al. 1998) shown in Additional file 1: Table S1. A point source having a mechanism of (strike, dip, rake) = (12, 81, − 89) (USGS 2022) was assumed at a depth of 598.1 km. The synthetic seismograms were obtained with a discrete wavenumber method (Bouchon 1981). The result is shown in Additional file 1: Figure S1. A very distinct S wave arrives approximately 130 s after the P wave arrival. There is no prominent arrival except for the S wave in the latter part of the seismogram. Therefore, it is clear that the later portions of the paste up shown in Fig. 3 shows the response of the sediment to an incident S wave. Therefore, it is appropriate to use the later portions to evaluate site amplifications. Additional file 1: Figure S1 also shows that the incident waves are similar between SOYH01 and NMRH03 because of the large hypocentral distance. Therefore, it is reasonable to assume that the difference of ground motions at different stations represents the difference of the site effects in the region shown in Fig. 3.

In the following, we will focus on the stations that recorded S waves. Figure 4 shows the observed Fourier spectra for the May 24, 2013 Sea of Okhotsk earthquake. The Fourier spectra were calculated for the S wave part for the K-NET and KiK-net records at the ground surface. For the stations that recorded both P and S waves, the record was divided into the P and S wave parts using a cosine taper and the latter was used. In each panel, the spectrum at ABSH05 is plotted for reference, because, according to the GIT analysis, this was the station with the smallest site amplification among the stations that recorded the S waves of the May 24, 2013 Sea of Okhotsk earthquake (the location of ABSH05 is shown in Fig. 1b). At stations such as SOYH01, SOYH02, HKD004 and RMIH01 (the locations are shown in Fig. 1b), the Fourier spectra at low frequencies are significantly larger compared to ABSH05. At stations such as SOYH08, SOYH09 and SOYH10, the Fourier spectra at low frequencies are still larger compared to ABSH05. At southern stations, such as KKWH02 and ABSH02, the low-frequency Fourier spectra approach to that of ABSH05.

Figure 5 shows the site amplification factors at strong motion stations. At each station, two site amplification factors are compared. One is the result of the GIT analysis (Nozu and Sugano 2010). The gray hatching indicates the average ± one standard deviation in the logarithmic scale except for HKD004, SOYH09 and ABSH02, where only one record was available in the GIT analysis. The other is the site amplification factor based on the records of the May 24, 2013 Sea of Okhotsk earthquake. The observed Fourier spectrum at each station (Fig. 4) was divided by the observed Fourier spectrum at ABSH05 and multiplied by the site amplification factor at ABSH05 evaluated by Nozu and Sugano (2010). At stations, such as SOYH01, SOYH02, HKD004 and RMIH01, the site amplification factor at low frequencies exceeds 20. Among these stations, SOYH01, SOYH02 and HKD004 are located along the coast of Hokkaido facing the Sea of Okhotsk. Therefore, from this figure, we can make sure that the region of large site amplification in the low-frequency range in Northern Hokkaido does extend to the eastern Soya region. In this figure, the emphasis is on the fact that the large site amplification is indicated from both the GIT analysis and the records from the May 24, 2013 Sea of Okhotsk earthquake. The author is not necessarily expecting that they result in exactly the same amplification factor, because the amplification factor may depend on the incident angle of the S waves.

Figure 1b shows the comparison between the J-SHIS model and the site amplification factors at strong motion stations based on the records of the May 24, 2013 Sea of Okhotsk earthquake (Fig. 5). The color contour is the same as Fig. 1a and indicates the thickness of the layers with a shear wave velocity less than 2000 m/s in the J-SHIS model. Blue, yellow and red circles are used similarly as in Fig. 1a. The results clearly indicate that the region of large site amplification in the low-frequency range in Northern Hokkaido extends to the eastern Soya region ,where the J-SHIS model does not indicate the existence of thick sedimentary layers.

The May 24, 2013 Sea of Okhotsk earthquake is unique in terms of its size and distance and it was difficult to find another earthquake that allows us to conduct a similar analysis in the same region. For example, for the May 30, 2015, M_W7.9, Ogasawara earthquake, only P wave part was recorded at the stations shown in Fig. 4 except for ABSH05, where only S wave part was recorded. Thus, a similar analysis is prohibitive for this event. The only exception could be the June 29, 2002, M_W7.1, Vladivostok earthquake shown in Fig. 2. For this earthquake, only P

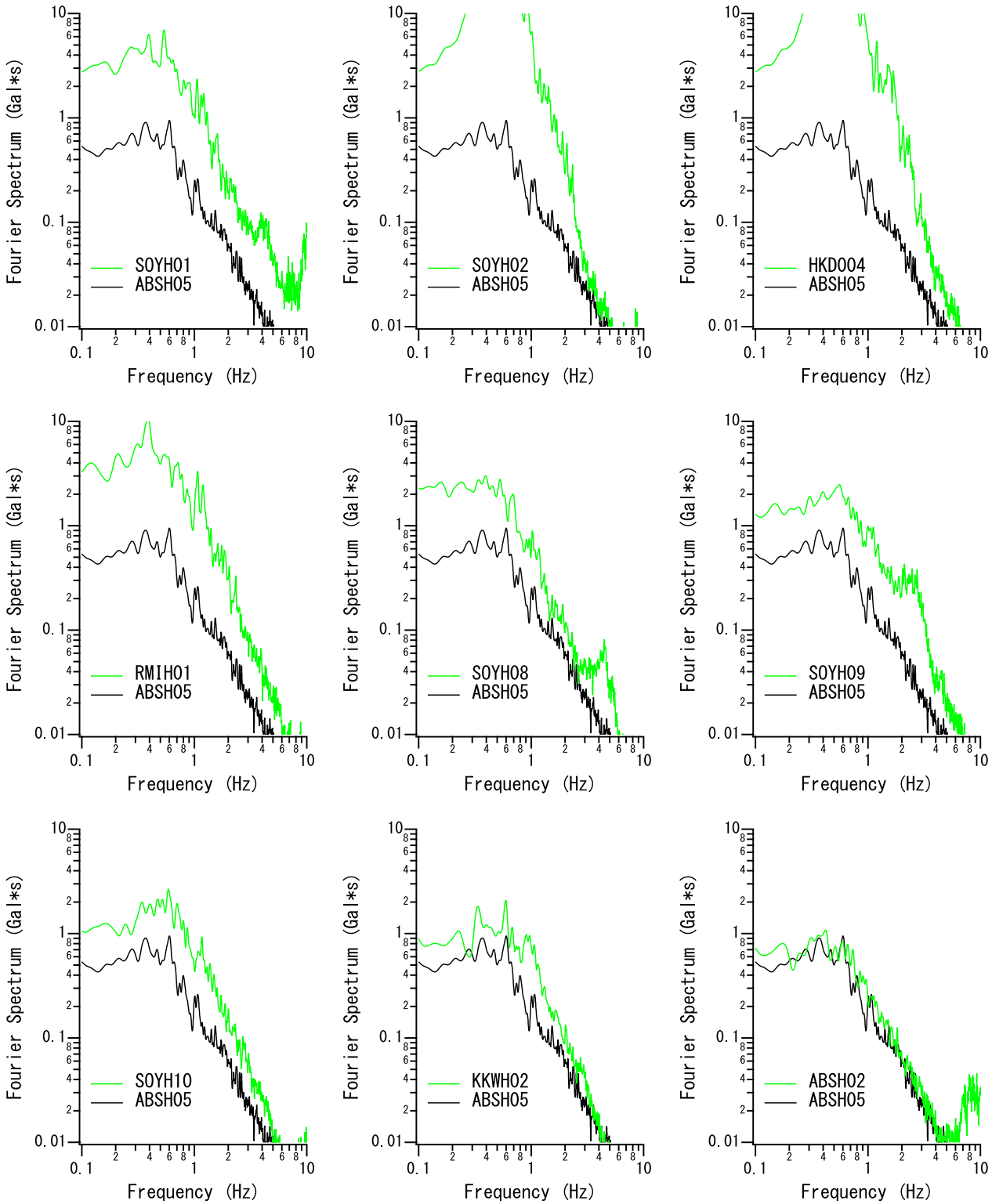

Fig. 4 Observed Fourier spectra for the May 24, 2013 Sea of Okhotsk earthquake; The Fourier spectra were calculated for the S wave part for the K-NET and KiK-net records at the ground surface. For the stations that recorded both P and S waves, the record was divided into the P and S wave parts using a cosine taper and the latter was used. The square root of the squared sum of two horizontal components is shown. A Parzen window with a band width of 0.05 Hz was applied. In each panel, the spectrum at ABSH05 is plotted for reference

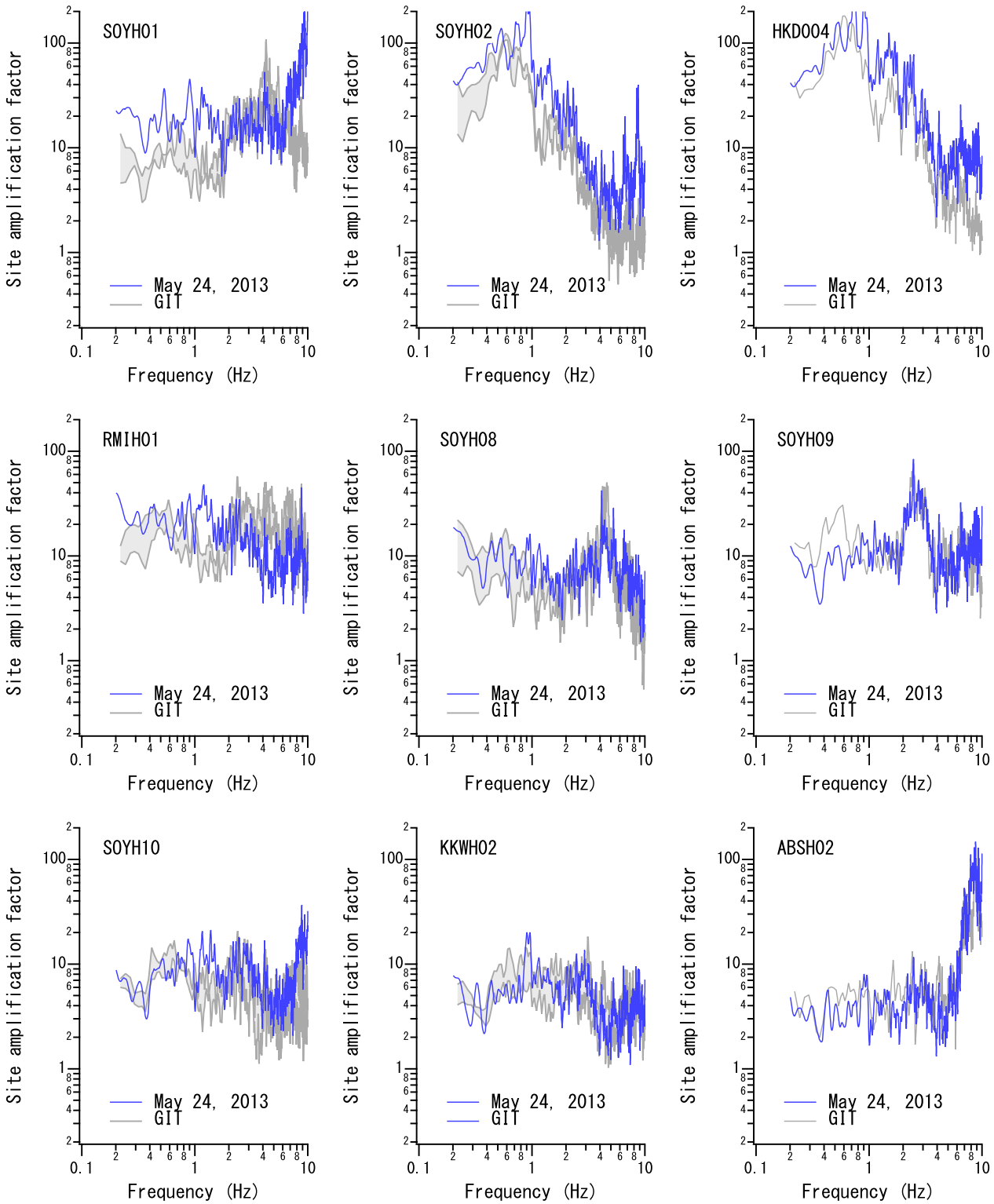

Fig. 5 Site amplification factors at strong motion stations; At each station, two site amplification factors are compared. One is the result of the GIT analysis (Nozu and Sugano 2010). The gray hatching indicates the average ± one standard deviation in the logarithmic scale except for HKD004, SOYH09 and ABSH02, where only one record was available in the GIT analysis. The other is the site amplification factor based on the records of the May 24, 2013 Sea of Okhotsk earthquake (blue line). The observed Fourier spectrum at each station (Fig. 4) was divided by the observed Fourier spectrum at ABSH05 and multiplied by the site amplification factor at ABSH05 evaluated by Nozu and Sugano (2010)

wave part was recorded at all the stations shown in Fig. 4. Although it is not possible to discuss the site response to an incident S wave based on this event, it is still possible to compare the site response to an incident P wave. The results are shown in Additional file 1: Figures S2 and S3. Additional file 1: Figure S2 shows the Fourier spectra calculated for the P wave part for the K-NET and KiK-net records at the ground surface for the June 29, 2002 Vladivostok earthquake. Additional file 1: Figure S3 compares the site amplification factors based on the GIT analysis (Nozu and Sugano 2010) and those based on the records of the June 29, 2002 Vladivostok earthquake. The result does not disagree with the statement that the region of large site amplification in the low-frequency range in Northern Hokkaido extends to the eastern Soya region.

Conclusions and discussion

In this study, the records of the May 24, 2013, M_W8.3, Sea of Okhotsk earthquake were used to investigate the distributions of site amplification factors in Northern Hokkaido. Because this is a distant earthquake and the epicentral distance was greater than 1300 km even at the closest station in Hokkaido, it was assumed that the difference of ground motions at different stations represents the difference of the site effects. The author was especially interested in the site amplification factors in the east part of Northern Hokkaido, because the conventional GIT analysis (Nozu and Sugano 2010) resulted in large site amplification factors not only in the west part but also in the east part of Northern Hokkaido and their result was not consistent either with the CDMC map (2008) or the J-SHIS model.

The results of this study based on the records of the May 24, 2013 Sea of Okhotsk earthquake clearly indicates that the region of large site amplification in the low-frequency range in Northern Hokkaido does extend to the Okhotsk Coast. According to this result, it could be reasonable to anticipate the existence of thick sedimentary layers not only in the west part but also in the east part of Northern Hokkaido. However, existing velocity structure models do not suggest the existence of such layers.

One possible cause of the discrepancy between this amplification pattern and the existing velocity structure models could be that they are less constrained by deep boring surveys and seismic reflection surveys in the east part of Northern Hokkaido. The velocity structure model used to create the CDMC (2008) map was originally developed in the Hokkaido Working Group of the Investigating Committee for the Subduction Earthquakes along the Japan and Chishima Trench, Central Disaster Management Council (2004). In Hokkaido, many deep boring surveys and seismic reflection surveys were conducted by the Japan National Oil Corporation (JNOC). The deep boring surveys also included PS loggings. Therefore, the Hokkaido Working Group first developed a geological structure model and then converted it into a velocity structure model. When they constructed the geological structure model, they referred to the results of the deep boring surveys and seismic reflection surveys by JNOC. However, for the areas of less surveys, they relied on geological information. According to Figs. 2.1 and 2.2 of CDMC (2004), the deep boring surveys and seismic reflection surveys had been conducted by JNOC in the west part of Northern Hokkaido, but not in the east part, although there were offshore survey lines. Therefore, the velocity structure model of CDMC (2004) and CDMC (2008) was less constrained by the deep boring surveys and seismic reflection surveys in the east part. This could be the reason why the CDMC (2008) map does not capture the amplification of low-frequency ground motions in the east part of Northern Hokkaido. Similarly, the J-SHIS model (Fujiwara et al. 2009) was constrained by the deep boring surveys and seismic reflection surveys by JNOC in the west part of Northern Hokkaido, but in the east part of Northern Hokkaido, the model is less constrained.

It should be noted that the PS logging data at the KiK-net station SOYH07 (Aoi et al 2020) indicates the existence of a layer with a shear wave velocity of 2290 m/s at a depth of 128 m, which is consistent with existing velocity structure models. Because this station did not record S waves during the May 24, 2013 Sea of Okhotsk earthquake as shown in Fig. 3, this station was not included in the spectral analyses in Figs. 4 and 5. However, the relatively small P wave amplitude at SOYH07 (Fig. 3) may be indicating that this station is not necessarily representing the averaged characteristics in the eastern Soya Region.

So far, there is no clear explanation about the cause of the discrepancy between the site amplification pattern in the east part of Northern Hokkaido and the existing velocity structure models. It is desirable in a future study to reveal the cause of the discrepancy.

Abbreviations

CDMC	Central Disaster Management Council
JNOC	Japan National Oil Corporation
J-SHIS	Japan Seismic Hazard Information Station

Supplementary Information

The online version contains supplementary material available at https://doi.org/10.1186/s40623-023-01936-y.

Additional file 1: Table S1. Subsurface structure model by Fukuyama et al. (1998), which was used to calculate synthetic seismograms shown in Additional file 1: Figure S1. **Figure S1.** Synthetic seismograms calculated for the locations of SOYH01 and NMRH03 (Fig. 3) assuming a point source, using a layered subsurface structure model shown in Additional file 1: Table S1. A point source having a mechanism of (strike, dip, rake) = (12,

81, –89) (USGS 2022) was assumed at a depth of 598.1 km. The synthetic seismograms were obtained with a discrete wavenumber method (Bouchon 1981) and normalized so that the peak amplitude at SOYH01 is one. The synthetic seismograms are plotted for the EW component. **Figure S2.** Observed Fourier spectra for the June 29, 2002 Vladivostok earthquake; The Fourier spectra were calculated for the P wave part for the K-NET and KiK-net records at the ground surface. The square root of the squared sum of two horizontal components is shown. A Parzen window with a band width of 0.05 Hz was applied. In each panel, the spectrum at ABSH05 is plotted for reference. **Figure S3.** Site amplification factors at strong motion stations; At each station, two site amplification factors are compared. One is the result of the GIT analysis (Nozu and Sugano 2010). The gray hatching indicates the average ± one standard deviation in the logarithmic scale except for HKD004, SOYH09 and ABSH02, where only one record was available in the GIT analysis. The other is the site amplification factor based on the records of the June 29, 2002 Vladivostok earthquake (blue line). The observed Fourier spectrum at each station (Additional file 1: Figure S2) was divided by the observed Fourier spectrum at ABSH05 and multiplied by the site amplification factor at ABSH05 evaluated by Nozu and Sugano (2010). It should be noted that the Fourier spectra of the 2002 Vladivostok earthquake were evaluated based on the P wave part.

Acknowledgements
The author would like to thank the National Research Institute for Earth Science and Disaster Resilience for providing strong motion data.

Author contributions
AN did all the analysis and wrote the manuscript.

Funding
Not applicable.

Availability of data and materials
The strong motion data used in this study can be found at the website of the National Research Institute for Earth Science and Disaster Resilience,. The J-SHIS velocity structure model can be found at the J-SHIS website at https://www.j-shis.bosai.go.jp/en/.

Declarations

Ethics approval and consent to participate
Not applicable.

Consent for publication
Not applicable.

Competing interests
Not applicable.

Author details
[1]Director of Earthquake Disaster Prevention Engineering Department, Port and Airport Research Institute, 3-1-1, Nagase, Yokosuka 239-0826, Japan.

Received: 25 September 2022 Accepted: 17 November 2023
Published online: 30 November 2023

References

Aoi S, Asano Y, Kunugi T, Kimura T, Uehira K, Takahashi N, Ueda H, Shiomi K, Matsumoto T, Fujiwara H (2020) MOWLAS: NIED observation network for earthquake, tsunami and volcano. Earth Planets Space 72:126. https://doi.org/10.1186/s40623-020-01250-x
Bouchon M (1981) A simple method to calculate green's functions for elastic layered media. Bull Seismol Soc Am 71:959–971
Central Disaster Management Council (2004) On the deep subsurface structure model in Hokkaido. https://www.bousai.go.jp/kaigirep/chuobou/senmon/nihonkaiko_chisimajishin/hokkaido_wg/1/pdf/siryou_3_2.pdf. Accessed 23 Sep 2022
Central Disaster Management Council (2008) The predominant period of long-period ground motions and the natural period of deep subsoil. https://www.bousai.go.jp/kaigirep/chuobou/senmon/tounankai_nankaijishin/pdf/shiryou4.pdf. Accessed 23 Sep 2022
Fujiwara H, Kawai S, Aoi S, Morikawa N, Senna S, Kudo N, Ooi M, Hao KX, Hayakawa Y, Toyama N, Matsuyama H, Iwamoto K, Suzuki H, Liu Y (2009) A study on subsurface structure model for deep sedimentary layers of Japan for strong-motion evaluation. Technical Note of the National Research Institute for Earth Science and Disaster Prevention 337. https://www.j-shis.bosai.go.jp/map/JSHIS2/download.html. Accessed 23 Sep 2022
Fukuyama E, Ishida M, Dreger DS, Kawai H (1998) Automated seismic moment tensor determination by using on-line broadband seismic waveforms. Zisin, 2 Ser 51:149–156
Iwata T, Irikura K (1986) Separation of source, propagation and site effects from observed S-waves. Zisin,2 Ser 39:579–593
NIED (2022) F-net, Broadband Seismograph Network. https://www.fnet.bosai.go.jp/top.php?LANG=en. Accessed 23 Sep 2022
Nozu A, Nagao T (2005) Site amplification factors for strong-motion sites in Japan based on spectral inversion technique. Technical Note of the Port and Airport Research Institute 1112. https://www.pari.go.jp/PDF/no1112.pdf. Accessed 23 Sep 2022
Nozu A, Sugano T (2010) Site amplification factor for strong-motion sites in northern Hokkaido, Japan, based on spectral inversion technique. Technical Note of the Port and Airport Research Institute 1214. https://www.pari.go.jp/PDF/no1214.pdf. Accessed 23 Sep 2022
USGS (2022) Earthquakes. https://www.usgs.gov/programs/earthquake-hazards/earthquakes. Accessed 23 Sep 2022

Publisher's Note